J5.3

TESTING OF THE QUIC-PLUME MODEL WITH WIND-TUNNEL MEASUREMENTS FOR A HIGH-RISE BUILDING

Michael D. Williams[1], Michael J. Brown[1], David Boswell[1], Balwinder Singh[2], and Eric Pardyjak[2]
[1]Los Alamos National Laboratory, Los Alamos, NM and [2]University of Utah, Salt Lake City, Utah

1. Introduction

There is a growing concern about the threat of a malicious release of harmful substances to the air in order to cause harm to the population. In order to help decision-makers assess the consequences of such an attack, accurate predictions of the transport and dispersion of airborne contaminants in cities are needed. The complex flows produced by buildings pose difficult challenges to dispersion modelers. Among features of concern are channeling of plumes down street channels, circular transport within street canyon vortices, upwind transport, intermittent transport from street level to roof level within spiral vortices that develop on the downwind side of tall buildings, and the retention of toxic materials trapped between buildings.

A number of groups have developed computational fluid dynamics models that have been applied to neighborhood-scale problems and have explicitly resolved hundreds of buildings in their simulations. However, CFD models are computationally intensive and for some applications turn-around time is of the essence. For example, planning and assessment studies in which hundreds of cases must be analyzed or emergency response scenarios in which plume transport must be computed quickly. For many applications, where quick turn-around is needed (e.g., emergency response) or where many simulations must be run (e.g., vulnerability assessments), a fast response modeling system is required. Fast running models are not only needed for emergency response and post-event applications, but for scenarios in which many cases must be run or immediate feedback is needed.

We have developed the QUIC (Quick Urban & Industrial Complex) dispersion modeling system to fill that need. It can relatively quickly compute the dispersion of airborne contaminants released near buildings. It is comprised of QUIC-URB, a model that computes a 3D mass consistent wind field for flows around buildings (Pardyjak and Brown, 2001), QUIC-PLUME, a model that describes dispersion near buildings (Williams et al., 2003), and a graphical user interface QUIC-GUI (Boswell et al., 2004). The QUIC dispersion code is currently being used for building-scale to neighborhood-scale transport and diffusion problems with domains on the order of several kilometers. Figure 1 illustrates the modeled dispersion for a release in downtown Salt Lake City.

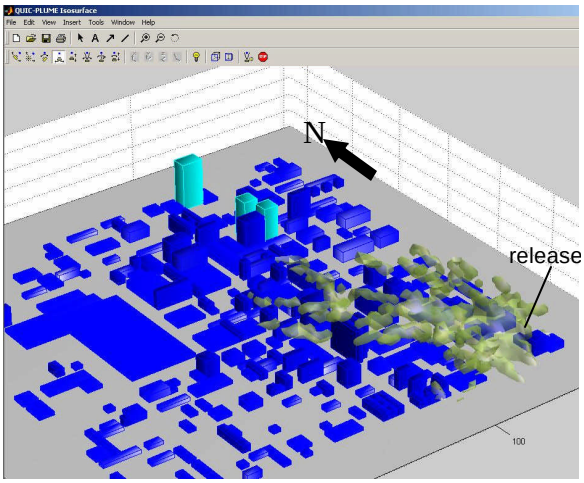

Figure 1. A QUIC simulation of plume dispersal in Salt Lake City under the influence of southeast winds. Shown are the estimated contaminant isopleths for a release near street level.

This paper describes the QUIC-PLUME random-walk dispersion model formulation, the turbulence parameterization assumptions, and shows comparisons of model-computed concentration fields with measurements from a single-building wind-tunnel experiment. It is shown that the traditional three-term random walk model with a turbulence scheme based on gradients of the mean wind performs poorly for dispersion in the cavity of the single-building, and that model-experiment comparisons are improved significantly when additional drift terms are added and a non-local mixing scheme is implemented.

2. Background

Several fast-response dispersion models of varying levels of fidelity have been developed to explicitly account for the effects of buildings. Several are intended for use around a single building so are not directly applicable to neighborhood-scale dispersion problems. Recently, several codes have been developed to treat these scales. The Urban Dispersion Model is a Gaussian puff model that utilizes simple algorithms for puff-building interaction (Hall et al., 2000). Although the model does not produce wind fields around buildings, it accounts for mixing in the lee of the building and some channeling effects.

* *Corresponding author address:* Michael D. Williams, LANL, D-4, MS F604, Los Alamos, NM 87545, mdw@lanl.gov.

Comparisons to concentration measurements from the URBAN 2000 tracer experiment performed in Salt Lake City showed reasonable agreement for many cases if local winds near the source are appropriately accounted for. A potential flow model called MIDAS-AT has been advertised for dispersion applications in urban areas (http://www.plg-ec.com/), however, we have not been able to obtain reports or open-literature publications. In principle, a potential flow model can produce velocity fields around groups of buildings, but with the restriction that the flow must be irrotational. It appears that the dispersion model is of a random-walk type.

Röckle (1990) developed a diagnostic mass consistent wind model for computing the 3D flow field around isolated buildings and groups of buildings. The model utilizes empirical algorithms for determining initial wind fields in the cavity, wake, and upstream recirculation zones for single buildings, but it also includes algorithms for velocity fields in between buildings. A mass consistent wind field is then produced similar to the approach used in traditional diagnostic wind modeling, except that special treatment of boundary conditions is needed at building walls. The computed wind field is not restricted to being irrotational as in potential flow models. Several different approaches have been used to compute the dispersion of airborne contaminants, including Eulerian finite difference methods and random-walk models (Kaplan and Dinar, 1996). Whatever solution method is used for obtaining the concentration fields, the approach for obtaining turbulence variables is of special importance given that the diagnostic wind model approach only provides mean wind fields.

The Röckle-style model has been evaluated for a handful of cases. For a street intersection defined by four adjacent courtyards, Röckle et al. (1998) showed reasonable agreement between model-computed wind fields and wind-tunnel measurements for various inflow wind angles. Kaplan and Dinar (1996) qualitatively compared the model solutions to CFD model results for flow around two and three buildings and to wind-tunnel measurements of concentration on street canyon walls. Using a wind-tunnel study of an industrial complex, Röckle (1990) found that the model-computed wind directions and wind speed agreed fairly well at several points within the complex for various inflow wind directions.

Surprisingly, the urban diagnostic wind model approach has not been extensively tested for the single building case. We have found one example, in which Gross et al. (1994) compared turbulent intensity predictions with a few measurements made downwind of a cube. To help resolve this deficiency, Pardyjak and Brown (2002) compared model-computed wind fields to centerline velocities measured in the USEPA meteorological wind tunnel (Snyder and Lawson, 1994) for rectilinear buildings of varying width, height, and downwind length with a prevailing wind normal to the building face. Bagal et al. (2003) evaluated the upstream rotor for a single building for several different aspect ratios. In this paper, we will evaluate the concentration fields produced by the QUIC model for a point-source release in uniform and shear flow, and for the case of a release in the lee of tall building.

3. Model Description

We will only briefly describe the QUIC-URB wind model in this paper. The underlying code is based on the work of Röckle (1990). It uses empirical algorithms and mass conservation to quickly compute the mean 3D flow field around building complexes. The size, shape, and velocity field for the upstream rotor, cavity, wake, and street canyon vortex are specified, and then a mass consistent wind field is produced similar to the approach used in traditional diagnostic wind modeling (e.g., Sherman, 1978), except that special treatment of boundary conditions is needed at building walls. Improvements to the original Röckle model are described in Bagal et al. (2003), Gowardhan (2003) and Pardyjak et al. (2003). Further details can be found in Pardyjak et al. (2004)

QUIC-PLUME uses a stochastic Lagrangian random-walk approach to estimate concentrations in a 3D gridded domain. The model is designed to use mean wind fields produced by the QUIC-URB model. Parcels, representing aerosols or gases, are transported with a vector sum of mean winds from QUIC-URB plus turbulent fluctuating winds computed using the random-walk equations. Turbulence parameters needed in the random-walk equations are estimated from vertical and horizontal gradients in the mean wind. A detailed description of the theory is described in a companion document (Williams and Brown, 2004).

3.1 Random-walk equations.

Lagrangian random-walk models describe dispersion by simulating the releases of air parcels and moving them with an instantaneous wind composed of a mean wind plus a turbulent wind. The equations that describe the parcel positions are:

$$x(t+\Delta t) = x(t) + \overline{U}\Delta t + \frac{u'(t+\Delta t) + u'(t)}{2}\Delta t \,, \qquad (1)$$

$$y(t+\Delta t) = y(t) + \overline{V}\Delta t + \frac{v'(t+\Delta t) + v'(t)}{2}\Delta t \,, \qquad (2)$$

and

$$z(t+\Delta t) = z(t) + \overline{W}\Delta t + \frac{w'(t+\Delta t) + w'(t)}{2}\Delta t \,, \qquad (3)$$

where *x, y,* and *z* are the longitudinal, lateral, and vertical position coordinates of the particle, $\overline{U}$, $\overline{V}$, and $\overline{W}$ are the x, y, and z components of the mean wind, u', v', and w' are the turbulent components of the instantaneous wind, and Δt is the time step.

The temporal evolution of the fluctuating components of the wind are calculated from:

$$u'(t+\Delta t) = u'(t) + du\,, \tag{4}$$

$$v'(t+\Delta t) = v'(t) + dv\,, \tag{5}$$

and,

$$w'(t+\Delta t) = w'(t) + dw\,. \tag{6}$$

Traditionally, a three term random-walk equation for the vertical velocity has been used in the air quality community for describing vertical dispersion (e.g., references):

$$dw = -\frac{C_o e}{2} l_{33} w' dt + \frac{1}{2}\left(1 + l_{33} w'^2\right)\frac{\partial t_{33}}{\partial z} dt + (C_o e dt)^{1/2} dW_3(t), \tag{7}$$

where the constant C_o is the universal constant for the Lagrangian structure function, e is the mean rate of turbulence kinetic energy dissipation, and $dW_3(t)$ is a random number generator with uncorrelated, normally distributed variables with mean of zero and standard deviation of one. The first term on the right is called the memory term, the second term is the drift term and the third term is the random acceleration term. Comparisons to plume dispersion experiments over flat surfaces have shown reasonable agreement. As we will show later, we have found poor agreement with the traditional random-walk equation for a release near the backside of a tall building. This is in part due to the assumptions that go into the derivation of equation (7) which do not hold for flows around buildings, namely the mean lateral and vertical winds $\overline{V}$ and $\overline{W}$ are zero and the mean horizontal winds are uniform (i.e., contain no gradients).

As reviewed by Rodean (1996), the general set of equations for du, dv, and dw can be derived from the Folker-Planck equations and the well-mixed condition and result in equations with a large number of terms. For the QUIC-PLUME model, we have taken a simplified form of the full set of equations and applied a local coordinate rotation in order to remove some of the approximations inherent in equation (7).

$$du = \left\{\frac{-C_o e}{2}\left[l_{11}u' + l_{13}w'\right] + \frac{\partial \overline{U}}{\partial z} w' + \frac{1}{2}\frac{\partial t_{13}}{\partial z}\right\} dt + \left\{\frac{\partial t_{11}}{\partial z}\left[l_{11}u' + l_{13}w'\right] + \frac{\partial t_{13}}{\partial z}\left[l_{13}u' + l_{33}w'\right]\right\}\frac{w'}{2} dt + (C_o e dt)^{1/2} dW_1(t), \tag{8}$$

$$dv = \left[-\frac{C_o e}{2}\left(l_{22}v'\right) + \frac{\partial t_{22}}{\partial z}\left(l_{22}v'\right)\frac{w'}{2}\right] dt + (C_o e dt)^{1/2} dW_2(t), \tag{9}$$

and

$$dw = \left\{-\frac{C_o e}{2}\left[l_{13}u' + l_{33}w'\right] + \frac{1}{2}\frac{\partial t_{33}}{\partial z}\right\} dt + \left\{\frac{\partial t_{13}}{\partial z}\left[l_{11}u' + l_{13}w'\right] + \frac{\partial t_{33}}{\partial z}\left[l_{13}u' + l_{33}w'\right]\right\}\frac{w'}{2} dt + (C_o e dt)^{1/2} dW_3(t), \tag{10}$$

where

$$l_{11} = \left(t_{11} - t_{13}^2 / t_{33}\right)^{-1}, \quad l_{22} = t_{22}^{-1},$$

$$l_{13} = \left(t_{13} - t_{11} t_{33} / t_{13}\right)^{-1}, \quad l_{33} = \left(t_{33} - t_{13}^2 / t_{11}\right)^{-1},$$

$$t_{11} = s_u^2, \quad t_{22} = s_v^2, \text{ and } t_{33} = s_w^2.$$

Note that the t's refer to kinematic stresses, i.e., shear or normal stress divided by density. A variety of investigators have estimated a plethora of C_o values ranging from 1.6 to 10 and we have chosen a value of 5.7 (e.g., Rodean, 1996).

3.2 Coordinate Rotation

The presence of buildings will produce non-zero lateral and vertical velocities and gradients in the horizontal wind. We partially account for this by using a local coordinate system for each particle as it travels along. This local coordinate system can change every time step and has the x-axis aligned with the mean wind vector and the z-axis normal to the mean wind vector in the direction of the largest gradient in the wind speed. The required axes rotations are shown below.

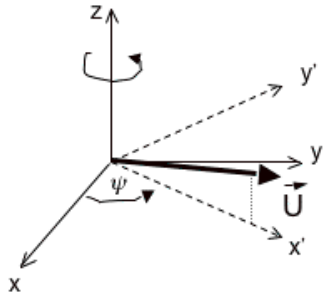

The first rotation aligns the x axis (now x') with the projection of the mean wind vector on the x-y plane by rotating about the z axis through the angle γ, where

$$\gamma = \arctan\left(\frac{v}{u}\right). \tag{11}$$

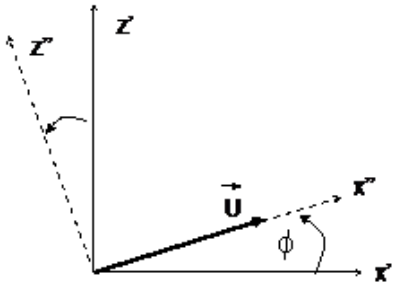

The second rotation aligns the x' axis (now x'') with the mean wind vector itself by rotating about the y' axis through the angle f where

$$f = \arctan\left(\frac{w}{\sqrt{u^2 + v^2}}\right). \qquad (12)$$

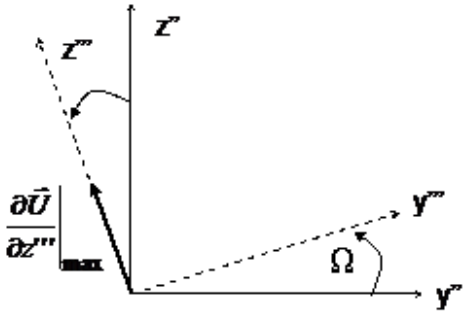

The third rotation occurs about the x'' axis (along the mean wind vector) and rotates the z'' (now z''') axis through the angle Ω into the direction of the largest gradient of mean velocity. The z''' axis is now in the direction in which the speed increases most rapidly in the plane normal to the wind direction. The angle Ω is calculated by optimizing the rate of change of the wind speed with respect to distance along the z''' axis,

$$\frac{\partial u'''}{\partial z'''} = \frac{\partial s}{\partial x}(\sin y \sin\Omega - \cos y \sin f \cos\Omega) - \frac{\partial s}{\partial y}(\cos y \sin\Omega + \sin y \sin f \cos\Omega) + \frac{\partial s}{\partial z}\cos f \cos\Omega \qquad (13)$$

with S the wind speed or u'''. The optimization results in the equation:

$$\Omega = \arctan\left(\frac{-\frac{\partial s}{\partial x}\sin y + \frac{\partial s}{\partial y}\cos y}{+\frac{\partial s}{\partial x}\cos y \sin f + \frac{\partial s}{\partial y}\sin y \sin f - \frac{\partial s}{\partial z}\cos f}\right) \qquad (14)$$

If the above equation results in a minimum rather than a maximum, the appropriate value is found by replacing Ω with $\Omega + p$.

3.3 Specification of turbulence variables.

The random-walk equations (8) – (10) require approximations for the normal and shear stresses and turbulent dissipation as a function of x, y, and z. The QUIC-URB wind model only provides a mean wind field. One straight-forward option is to use simple approximations for the turbulence terms using gradient transport and similarity theory. We have started with the traditional surface layer similarity relationships

$$s_u = 2u_*, \quad s_v = 2u_*, \quad s_w = 1.3u_*,$$

$$e = \frac{u_*^3}{k(z + z_0)}, \text{ and } t_{13} = -\langle u'w' \rangle = u_*^2, \qquad (14)$$

with z_0 the roughness length and $k=0.4$ the von Karman constant. Although these relationships have been show to approximately hold true above building rooftops, we are aware that they may not hold in and around building complexes. Preliminary analyses of experimental data in wind-tunnel and field experiments suggest that they may be accurate to within 50% when one treats u* as the local friction velocity, a function of x, y, and z. The relationship between the Reynolds shear stress and the normal stresses will be a topic of further research.

The key parameter for the estimation of the turbulence variables is the friction velocity u*. We consider u* to be the local friction velocity equal to the square root of the Reynolds shear stress and calculate it's magnitude based on gradient transport theory:

$$u_*(x,y,z) = l_z\left|\frac{\partial \bar{U}}{\partial z}\right| = k(z - z_{sfc})\left|\frac{\partial \bar{U}}{\partial z}\right|, \qquad (15)$$

with the mixing length l_z being the height above the surface (either the roof or ground) multiplied by the von Karman constant k. These relationships are applied to the rotated coordinate system rather than the unrotated coordinate system.

Where there are recirculating eddies or flow reversals, we compute an alternate mixing length that does not depend on the distance to a surface, but rather is indicative of the size of the eddy:

$$l_z = k\left(\frac{u}{\left|\frac{\partial u}{\partial z}\right|}\right). \qquad (16)$$

The smaller of the two expressions for the mixing length is then chosen for the computation of u*. The kinematic normal stresses are:

$$t_{11} = s_u^2 = t_{22} = s_v^2 = 4u_*^2;\ t_{33} = 1.69u_*^2, \quad (17)$$

while the kinematic Reynolds shear stress, t_{13}, and the dissipation, ε, are:

$$t_{13} = l_z \frac{\partial u}{\partial z}, \quad e = \frac{u_*^3}{l_z}. \quad (18)$$

Similar expressions are made for l_y with horizontal gradients replacing vertical gradients. The smaller of the length scales is used for the dissipation. (Williams, et. al., 2002). Currently, we are assuming an analogy between the treatment of wall-induced shear and vortex-based shear. However, this analogy may not hold because length scales are limited in size by walls in the former case, but not in the latter. Hence, we may be overestimating dissipation in vortex-based shear.

3.4 Turbulence due to Non-Local Mixing.

The initial version of the code performed poorly when applied to building dispersion problems and a number of modifications were made. The most significant was incorporation of provisions for non-local mixing. Smoke visualization in wind tunnels, as well as large-eddy simulations, of flows around buildings exhibit eddies that sweep contaminants across the cavities and wakes of buildings. Concentration measurements for releases in the building cavity suggest that there is considerable mixing in the lee of the building. Similar to daytime convective mixing in the atmospheric boundary layer, gradient mixing cannot account for this large eddy transport.

A non-local mixing scheme was implemented into the code in order to account for the large-eddy mixing in the wake of buildings. This process was conceptualized as driven by velocity differences between the winds passing by the sides of buildings and the light winds within the cavity. Two situations were considered: mixing produced by vertical-axis eddies that transports materials horizontally and mixing produced by horizontal-axis eddies that bring material down from the higher winds above the cavity or wake. A "non-local" friction velocity is then computed based on these velocity differences inside and outside of the canyon:

$$u_{*NL} = c \cdot \max(\Delta u_H, \Delta u_V)$$

where *c* has currently been chosen as the von Karman constant and *H* and *V* refer to the horizontal and vertical directions.

A mixing length scale needs to be defined in order to compute the velocity differences *Du*. In the case of horizontal mixing, the length scale l_{NLh} was chosen as the half-width of the wake or cavity and the velocity difference was calculated by comparing the winds at the edge of the building with those along the centerline of the wake or cavity. For vertical mixing, the length

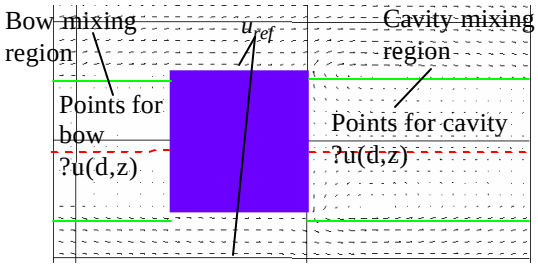

Figure 2. Sketch of geometry for non-local mixing showing the points used for u_{ref} and ?u.

scale l_{NLv} is the height of the building and the velocity difference is computed from the wind speed directly above the point of interest outside the cavity and that at the ground or rooftop. The non-local component of the normal and shear stresses are then computed as in eqns. 14. The stresses obtained by this approach are in the rotated coordinate system, so that they have to be transformed back into the original coordinate system.

3.5 Treatment of reflection by walls

Reflection of particles off of building walls and street surfaces is analogous to billiard ball type reflection. The code computes the penetration into the surface and reflects the particle appropriately. The case of multiple reflections at corners where walls and street meet is also accounted for. More information on the reflection scheme can be found in Williams and Brown (2004).

3.6 Concentration estimation

Average concentrations, normalized to unit release, are estimated by summing over all particles that are found within the sampling box *i,j,k* during the concentration averaging time t_{ave}:

$$c_{i,j,k} = \sum \frac{Q\Delta t_c}{n_{tot}\, dx_b dy_b dz_b t_{ave}},$$

where n_{tot} is the total number of particles released during the computations, dx_b, dy_b, and dz_b are the x, y, and z dimensions of the sampling box, respectively, and Δt_c is the particle time step.

4. Model Evaluation

A wind-tunnel experiment of dispersion in the vicinity of tall building was performed in the USEPA meteorological wind tunnel (Ohba et al., 1993). As shown in Fig. 3, a small spherical source was located near the surface on the downwind side of the building. Concentration measurements were made on the backside of the building and in the x-z vertical plane passing through the building centerline. Velocity measurements were also made in an x-z vertical plane and an x-y horizontal plane.

The wind-tunnel test section was 3.76 m wide, 2.16 m high, and 18.36 m long. The building base was 0.2 by 0.2 meters with a height of 0.6 meters. A simulated atmospheric boundary layer of ~2 m depth was generated in the wind-tunnel by using triangular fins mounted near the entrance to the test section and surface roughness elements on the test section floor. The freestream wind speed was set to 3.5 ms^{-1} for the wind-tunnel study such that the building Reynolds number was well above Reynolds number similarity.

We performed our simulations at full scale, such that the building had a base of 12 by 12 meters and was 36 meters tall. We modeled a release at 3 meters above ground and 6 meters behind the back wall. The release was simulated as particles released randomly from the surface of a sphere of radius 0.3 meters. Concentrations were non-dimensionalized for comparison purposes.

This is a particularly challenging geometry because of the rapid variations in the mean wind that are found in the wake of the building. In the vicinity of the source release location, winds are very light making generation of turbulence difficult from a modeling perspective. In addition, wall-effects play a major role in the transport and diffusion of the release such that near-wall parameterizations in the model will be tested as well.

Our comparisons to the experimental data were performed running QUIC-PLUME in two different modes. The local gradient mode computes u* based on local wind gradients, uses a coordinate rotation scheme aligned with the local mean wind at the particle position, and has no non-local mixing component. The non-local mixing mode is equivalent to the local gradient mode except that a non-local mixing scheme has been added in the calculation of u*.

The addition of non-local mixing resulted in much better agreement between measurements and the model-computed concentration fields on the back wall (Figs. 4-6). Figure 4 shows the measured concentrations on the back wall of the high rise building. With local mixing only (Fig. 5) the model dramatically underpredicts mixing in the cavity resulting in concentrations that are vastly overpredicted. Figure 6 shows that non-local mixing dramatically alters the computed concentration field and agrees much better

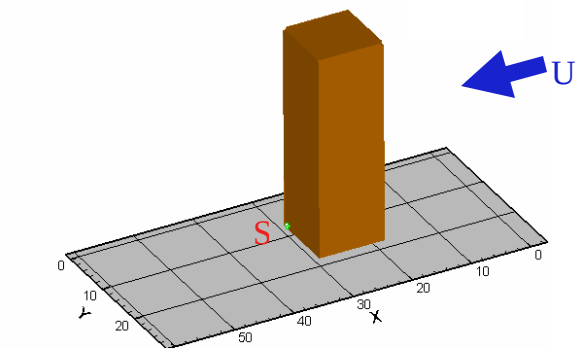

Figure 3. Modeled geometry for high-rise experiment.

with the measurements. The highest measured concentrations at the back wall are 116 normalized, while the normalized concentration for the local-gradient simulation is 6144. The non-local simulation produces a normalized, back wall maximum concentration of 177.

Approximately 70% of the simulated concentrations with the non-local mixing model are within a factor of two of the measurements. The agreement in lateral distribution nearest the height of the source is good as shown in Figure 7. The model tends to overpredict the near ground level concentrations by about 50% maximum as shown in Figure 8. The model underpredicts the measurements at heights of a few times the source height as shown in Figure 9. The largest discrepancies are near the sides of the building.

Comparison of model results and experimental measurements along the x-z centerplane downstream of the building are shown in Figs. 10-12. Figure 10 depicts contours of the measured normalized concentrations along the x-z centerplane, while Figs. 11 and 12 show the model-computed concentrations produced with non-local mixing and local-mixing, respectively. The local-mixing simulations provide a much more compact plume with much higher concentrations than the measured ones, indicating that turbulent mixing is underestimated in the cavity. The non-local mixing option, which effectively adds more turbulent mixing, produces much improved dispersion estimates.

Once again there is generally good agreement between the non-local simulations and the measurements with almost 80% of the simulations within a factor of two of the measurements. Near the source, there are some significant differences however. A comparison of the measured and model-computed vertical profiles at the back wall, near the back wall, and just downstream of the source are shown in Figs. 13-15. Figures 13 and 14 both show an elevated concentration maximum for the experimental measurements, while the model has the maximum at the ground. This indicates that as the contaminant is transported towards the back wall from the source, the model overpredicts vertical mixing. Figure 15 shows

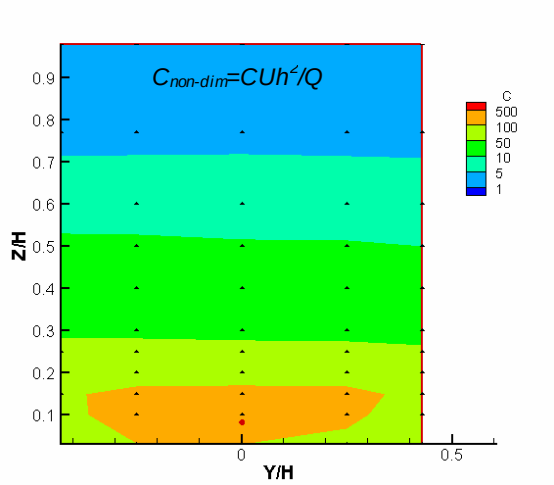

Figure 4. Measured, normalized concentrations on the backwall of a high-rise. Red dot indicates the source location while black dots show measurement locations.

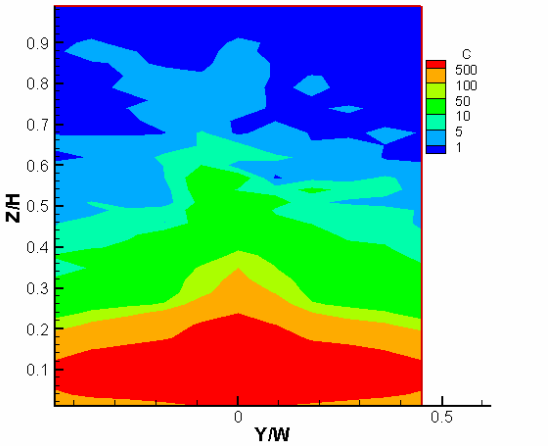

Figure 5. QUIC-computed normalized concentrations on the back wall of a high-rise using local mixing only.

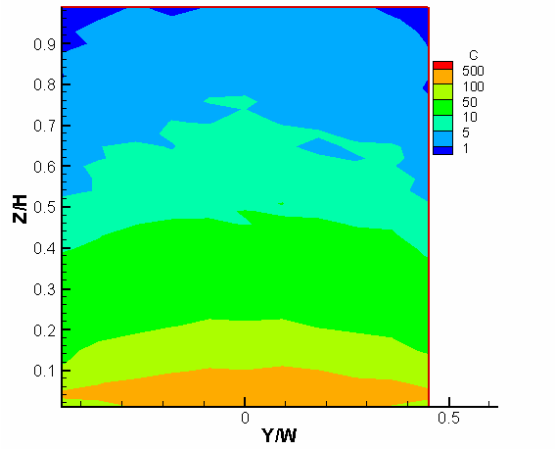

Figure 6. QUIC-computed normalized concentrations on the back-wall using non-local and local mixing.

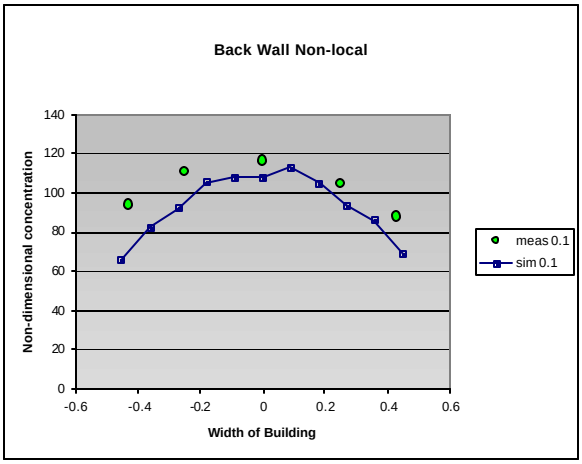

Figure 7. Comparison between measurements and calculations along the back wall at the approximate source height (QUIC with non-local mixing).

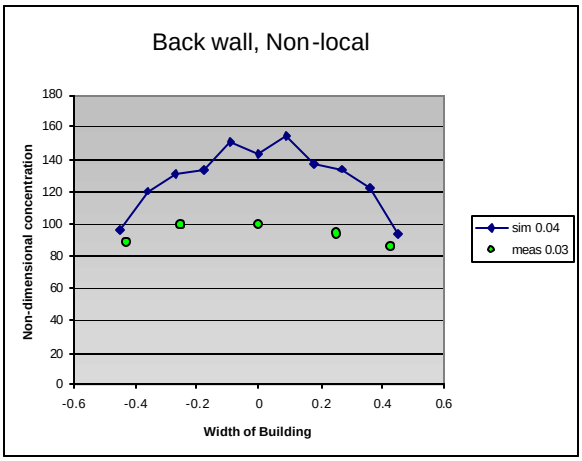

Figure 8. Comparison between measurements and calculations at a height near the ground on the backwall of a highrise (QUIC with non-local mixing).

.

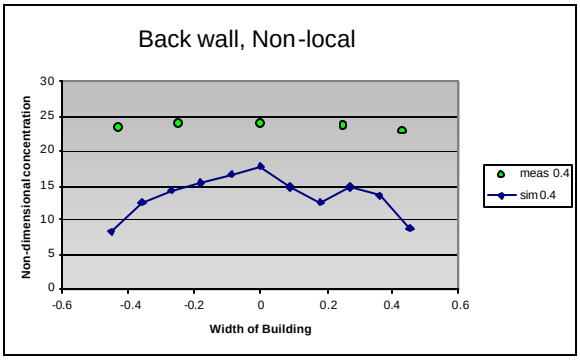

Figure 9. Comparison between measurements and calculations at a height equal to about five times the source height (QUIC with non-local mixing).

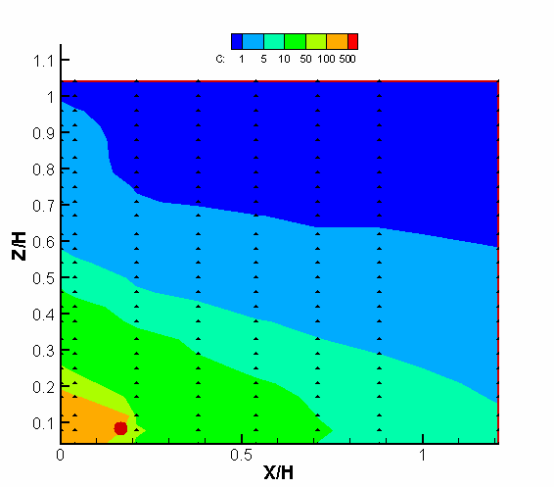

Figure 10. Measured, normalized concentrations along the downwind x-z plane behind the high-rise building. The red dot indicates the location of the source while the black dot indicates the measurement locations.

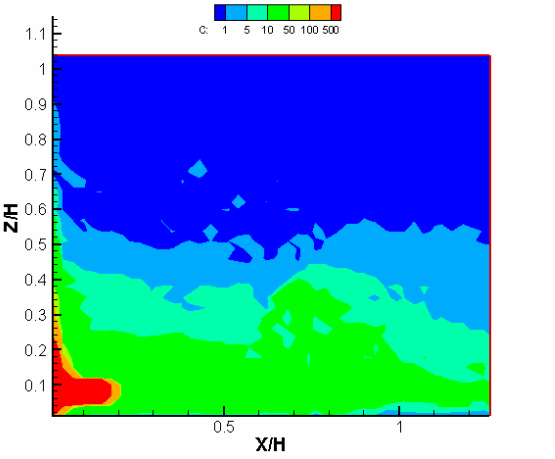

Figure 11. QUIC-computed normalized concentrations along the downwind x-z plane with local mixing only.

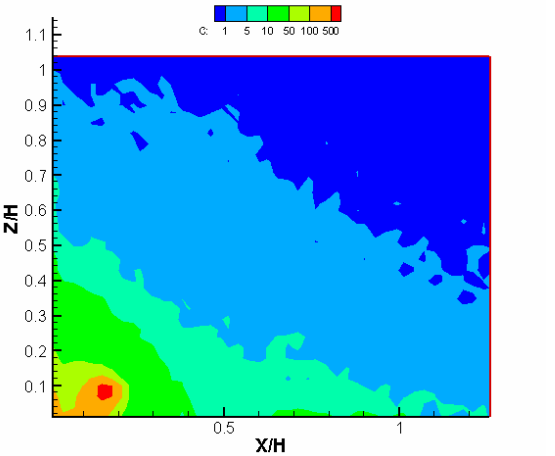

Figure 12. QUIC-computed normalized concentrations along the downwind x-z plane with the local and non-local mixing.

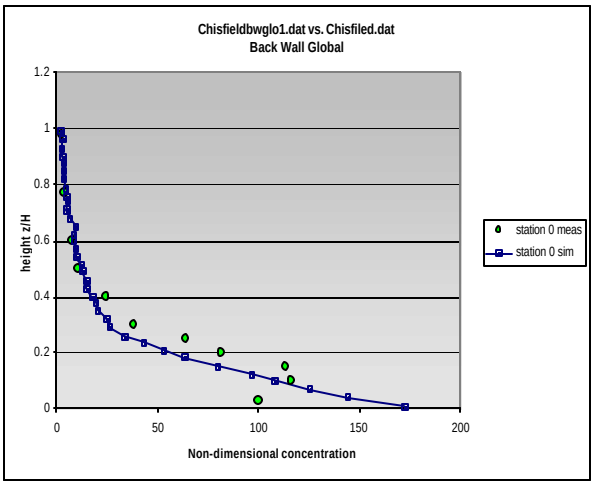

Figure 13. Comparison of measured (green circles) and QUIC model-computed vertical concentration profiles at the back wall (x/H=0). QUIC with non-local mixing.

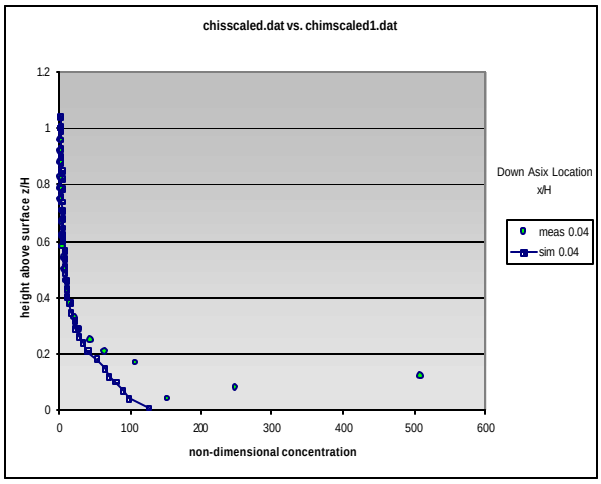

Figure 14. Comparison of measured and QUIC model-computed vertical concentration profiles near back wall (x/H=0.04). QUIC with non-local mixing.

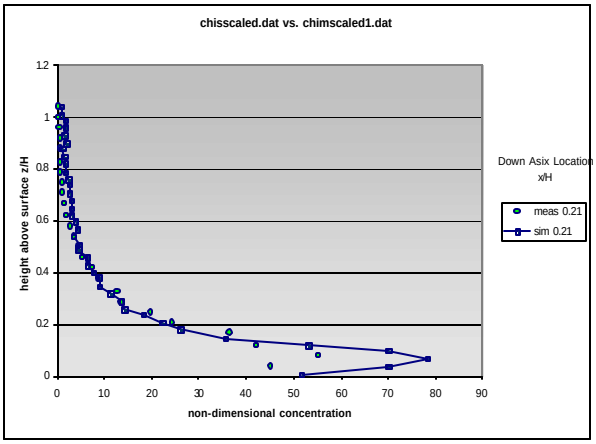

Figure 15. Comparison of measured and QUIC model-computed vertical concentration profiles at x/H=0.21. QUIC with non-local mixing.

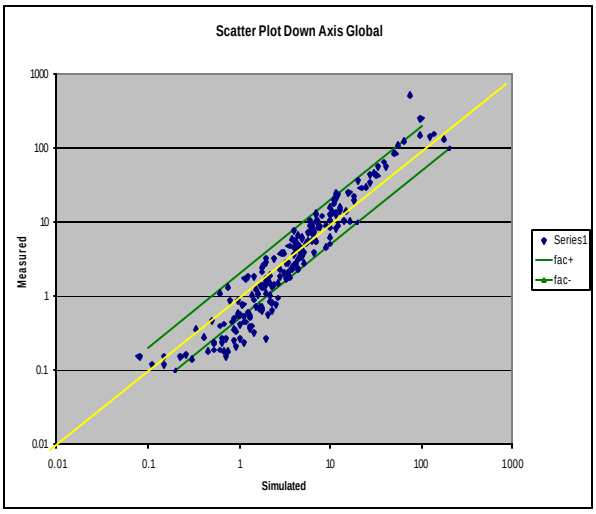

Figure 16. Scatterplot of measurements and QUIC-computed concentrations along the x-z centerplane downwind of the building. QUIC with **non-local** mixing.

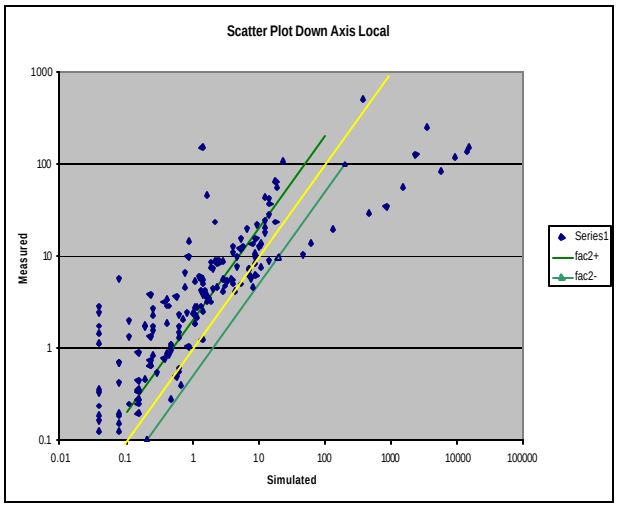

Figure 17. Scatterplot of measurements and QUIC-computed concentrations along the x-z centerplane downwind of the building. QUIC with **local** mixing only.

that both the measurements and the model have an elevated maximum at a location farther downwind (larger x/h), however, the model overpredicts the concentration by about 50 percent. Since the mean wind at this location is towards the back wall, this overprediction of the elevated maximum is not due to transport, but over mixing in the model.

Although there are some deficiencies near the source, the QUIC model with non-local mixing performed much better than the version with only local mixing. Scatter plots of paired-in-space comparisons on the down-axis vertical plane for non-local and local mixing options illustrate this point (Figs. 16 and 17, respectively). Local mixing results in significant over and under predictions. Non-local mixing results in 80% of the concentrations within a factor of two (green lines). Most of the discrepancies occur at very low concentrations where the model over predicts and at higher concentrations where the model tends to under predict.

5. Conclusions

The QUIC-PLUME model has been developed to provide a fast-running dispersion model that explicitly represents buildings. It uses QUIC-URB wind fields and describes turbulence and dispersion of airborne contaminants. It uses an enhanced random-walk methodology that is designed to describe transport in a complex environment with buildings. It also includes a non-local mixing formulation that better describes the turbulent mixing that occurs in building wakes or cavities.

We have tested the model against wind-tunnel measurements of a release near the back wall of a high-rise building. The measurements show that the material drifts towards the back wall before it spreads in the down axis direction. Despite the severe nature of this test the model performed well with the vast bulk of the simulations lying within a factor of two of the measurements along the back wall and in a plane extending along the axis of the building in the downwind direction. There are some discrepancies, however: (1) the model-computed concentrations show higher concentrations near the ground, (2) the model-computed concentrations fall off more rapidly in the transverse direction on the back wall, and (3) the model overpredicts mixing near the source.

When the QUIC-PLUME model was used without non-local mixing, it gave very poor results. The plume spread too slowly in the vertical and crosswind directions. This result was expected because of the very low wind speeds that occur in building wakes and cavities. When the turbulence is driven only by local gradients in wind speed, there is little turbulence calculated in building wakes and eddies. With non-local mixing acitivated, the QUIC-PLUME model is able to better replicate mixing in the cavity of the building.

7. References

Boswell, D. and M. Brown, 2004: QUIC Start Guide (v3.1) Quick Urban & Industrial Complex (QUIC) Dispersion Modeling System, Los Alamos National Laboratory.

Gowardhan, A., 2003: QUIC-URB validation study for 3D cubical building array, Univ. of Utah Technical Report, 8 pp.

Hall, D., A. Spanton, I. Griffiths, M. Hargrave, S. Walker, 2000: The UDM: A model for estimating dispersion in urban areas, Tech. Report No. 03/00 (DERA-PTN-DOWN).

Ohba, M., W. H. Snyder and R. E. Lawson, 1993: "Study on Prediction of Gas Concentrations Around Twin High-Rise Buildings using Wind-Tunnel Techniques, USEPA

Pardyjak, E.R., N. L. Bagal and M. J. Brown, 2003: Improved velocity deficit parameterizations for a fast response urban wind model, AMS Conf. on Urban Zone, Seattle, WA, LA-UR-03-8512.

Pardyjak, E. and M. Brown, 2002: Fast response modeling of a two building urban street canyon, 4th AMS Symp. Urban Env., Norfolk, VA, May 20-24 2002, LA-UR-02-1217.

Pardyjak, E. and M. Brown, 2001: Evaluation of a fast-response urban wind model – comparison to single-building wind-tunnel data, Int. Soc. Environ. Hydraulics, Tempe, AZ, Dec. 2001, LA-UR-01-4028, 6 pp.

Röckle, R., 1990: Bestimmung der Stomungsverhaltnisse im Bereich komplexer Bebauungsstrukturen. Ph.D. thesis, Vom Fachbereich Mechanik, der Technischen Hochschule Darmstadt, Germany.

Rodean, Howard C., 1996: "*Stochastic Lagrangian Models of Turbulent Diffusion,"* The American Meteorological Society, 82 pages.

Williams, M. D. and M.J. Brown, 2003: Description of the QUIC-PLUME Model, Los Alamos National Laboratory, LA-UR- 03-1426.

Williams, M. D., M. J. Brown, B. Singh, and D. Boswell, 2004: QUIC-PLUME Theory Guide, Los Alamos National Laboratory, LA-UR-04-0561.